On Topological Aspects of Ideal Fluid Flow and a Concomitant Singularity

P. Mulser
Institut für Angewandte Physik, Technische Hochschule Darmstadt

Z. Naturforsch. **42 a**, 1147–1153 (1987); received July 17, 1987

Dedicated to Professor Dieter Pfirsch on his 60th Birthday

The meaning of the trajectory of a fluid element in the Lagrangian picture of fluid dynamics for neutral and charged particles is clarified and it is shown that the homeomorphism induced by the flow has some very general topological properties. Consequences on void closure and thermalization in impact experiments are illustrated.

1. Introduction

The dynamics of a dense fluid can be described by subdividing it into small convex volume elements $\Delta\tau$ and by summing up the long range or field forces as well as the short range surface forces acting on each element. As the dimensions of $\Delta\tau$ are reduced it happens that any extensive quantity α of the mass enclosed, like momentum, energy, entropy, and the mass itself, becomes (I) nearly proportional to $\Delta\tau$ and (II) insensitive to moderate deformations of its shape (e.g. spheres instead of cubes for $\Delta\tau$). Let $\Delta\tau_0$ be such a suitable volume element. Then by determining the macroscopic quantities under consideration in $\Delta\tau_0$ for an adequate number of positions $\boldsymbol{x}_v$ in space and interpolating for all other positions $\boldsymbol{x}$ a well defined distribution $\alpha = \alpha(\boldsymbol{x}, t)$ results. The long range forces $\boldsymbol{f}(\boldsymbol{x}, t)$ are forces of gravitational or electromagnetic type and are proportional to the particle densities. The surface forces originate from binary or multiple collisions; their typical range is one mean free path λ and they are expressible in terms of a pressure tensor $\overleftrightarrow{\pi}$ or a scalar pressure p for which an equation of state in the form $p = p(\varrho, T)$ is assumed to exist. With these two kinds of forces Newton's 2nd law assumes the form of Euler's field equation for momentum balance,

$$\varrho \frac{\mathrm{d}\boldsymbol{v}}{\mathrm{d}t} = -\nabla\overleftrightarrow{\pi} + \boldsymbol{f}. \tag{1.1}$$

Reprint requests to Prof. Dr. P. Mulser, Institut für Angewandte Physik, Technische Hochschule Darmstadt, Hochschulstraße 2, D-6100 Darmstadt.

Solving this equation and integrating

$$\frac{\mathrm{d}\boldsymbol{x}}{\mathrm{d}t} = \boldsymbol{v}(\boldsymbol{x}, t) \tag{1.2}$$

for all initial positions $\boldsymbol{x} = \boldsymbol{a}$ at $t = t_0$, the flow field $\boldsymbol{v} = \boldsymbol{v}(\boldsymbol{a}, t)$ and the trajectories $\boldsymbol{x} = \boldsymbol{x}(\boldsymbol{a}, t)$ of all material points $\boldsymbol{a}$ in the Lagrangian description follow [1].

From a mathematical point of view fluid flow represents a one-parameter mapping, induced by (1.1) and (2.1), of one region of space onto another one, a pair of points $\boldsymbol{a}$ and $\boldsymbol{x}(\boldsymbol{a}, t)$ being connected by the trajectory of, let us say for the moment, the associated volume element (Figure 1). In four-dimensional space (space-time) due to the Lagrangian description events $(\boldsymbol{a}, t)$ are mapped onto events $(\boldsymbol{x}, t)$ along the world lines. $\boldsymbol{x}(\boldsymbol{a}, t)$ can be assumed to be piecewise continuously differentiable with respect to $\boldsymbol{a}$ and t. As long as the fluid density ϱ remains finite, different material points cannot merge into one since mass conservation states

$$\varrho(\boldsymbol{a}, t_0) = \varrho(\boldsymbol{x}, t) \cdot J(\boldsymbol{x}, \boldsymbol{a}, t)\,. \tag{1.3}$$

Thus, the Jacobian $J = |\partial(\boldsymbol{x})/\partial(\boldsymbol{a})|$ differs from zero everywhere. Mathematically, this fact is expressed by the property that $\boldsymbol{x}(\boldsymbol{a}, t)$ has to be a continuous one-to-one (biunique) correspondence or, in short, $\boldsymbol{x}(\boldsymbol{a}, t)$ is a topological mapping or homeomorphism [2, 3].

In a dense fluid $\lambda \ll (\Delta\tau_0)^{1/3}$ holds. As a consequence each fluid element is occupied by almost the same particles over a long distance and a curve $\boldsymbol{x}(\boldsymbol{a}, t)$ really describes the trajectory of the center of

0932-0784 / 87 / 1000-1147 $ 01.30/0. – Please order a reprint rather than making your own copy.

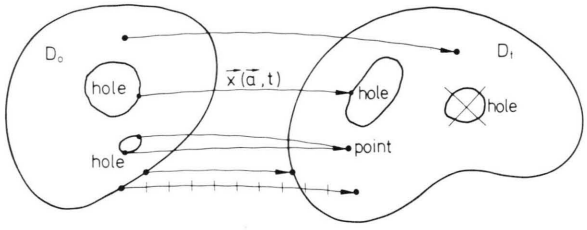

Fig. 1. Ideal fluid flow as a realization of a homeomorphism. Fluid flow implies a continuous one-to-one mapping of a domain D_0 onto a domain D_t. The homeomorphism induced by the trajectories $\boldsymbol{x}(\boldsymbol{a}, t)$ maps interior into interior and boundary into boundary points; the degree of connection is conserved.

mass of a fluid element. However, as the mean free path increases diffusion of particles is enhanced. In a neutral gas exhibiting collisions of mainly binary type the distinguishibility lifetime τ_1 of a "material point" is given by

$$\tau_1 = \frac{1}{4D}(\Delta\tau_0)^{2/3}, \quad D = \frac{1}{3}\langle v_{\text{th}}\,\lambda\rangle \tag{1.4}$$

with D being the diffusion coefficient. For instance, for air under standard conditions the lifetime of a cube $\Delta\tau_0 = (100\,\lambda)^3 = (10^{-3})^3\,\text{cm}^3$ is $\tau_1 = 1.5$ ms. With the diffusion of particles out of $\Delta\tau_0$, momentum and energy diffuse out also with transport constants

$$\eta = \varrho D, \quad \varkappa = c_v D,$$

in this way giving rise to an additional force term in the Euler equation (1.1) (viscosity) and an additional energy exchange term (thermal conduction) in the energy balance equation. c_v is the specific heat per unit volume at constant V. In neutral fluids the body force densities $\boldsymbol{f}(\boldsymbol{x}, t)$ are generally very smooth so that the shortest producible density scale is of the order of λ. For example, sound waves with $\lambda_s \lesssim 3\lambda$ cannot propagate. A subdivision of the fluid into volume elements smaller than λ does not lead to any additional fine-structure.

From such considerations on the lifetime of a material point one could be led to the conclusion that the usefulness of a fluid dynamic description should completely fail in the case of a system for which λ is of the order of the dimensions of the fluid. Surprising enough at first glance, this is not the case. One of the primary examples in this class of rarefied fluids is the collisionless plasma. There are important cases of laboratory plasmas for which the model of a collisionfree fluid is perfectly adequate and yet the correct equation of motion is again given by Euler's equation (1.1). This is easily verified by calculating the first moment of the collisionfree Boltzmann or Vlasov equation [4]. Since at each time instant (1.2) makes sense, also a Lagrangian description is again feasible and, as a consequence, the rarefied plasma flow mathematically also appears as a topological mapping. In nearly all cases of freely expanding plasma clouds the Lagrangian picture is used in numerical computations [5]. However there is a fundamental difference now: The mapping is no longer that of a physical i.e. material point. Owing to the reduced collision frequency all particles move through the volume elements on straight lines at the thermal speed of electrons or ions reducing in this way τ_1 of a material plasma point to the crossing time of an ion,

$$\tau_1 = \frac{(\Delta\tau_0)^{1/3}}{v_{\text{th},\,i}}.$$

On the other hand, the smallest dimension of plasma structures is given by the Debye length λ_D,

$$\lambda_D = \left(\frac{\varepsilon_0 k T}{n_e e^2}\right)^{1/2}.$$

It also represents the lower limit of the fluid picture for any meaningful subdivision of the plasma, $(\Delta\tau_0)^{1/3} \gtrsim \lambda_D$. The physical reason for (1.1) still being applicable to plasma volume elements of much smaller dimensions than λ is that because of the collective response of the charged particles the interaction occurs now via the macroscopic electric fields produced by thermally induced charge separation. Only when the characteristic distances become smaller than λ_D the electric field cannot build up adequately and all structures below λ_D disappear (e.g. electron plasma waves, collisionless shock structures [6]). When $\lambda > (\Delta\tau_0)^{1/3}$ holds, the mapping $\boldsymbol{x}(\boldsymbol{a}, t)$ can no longer be visualized as fluid orbits or center of mass trajectories of volume elements; the only valid information the mapping yields is the direction and magnitude of the speed of the fluid element which at the time instant t is located in position $\boldsymbol{x}$. The real center of mass $(\boldsymbol{a}, t)$ generally follows a completely different and nearly unpredictable trajectory now.

In what follows, topological aspects and implications of ideal fluid flow which follow from (1.1) and (1.2) are studied, and it is shown that an unexpected singularity originates from them. To illustrate this, several cases of relevance for application are described.

2. Ideal Fluid Flow

The basic concept of this section is that of the trajectory of a volume element. As seen above, because of the finite lifetime τ_1 of material points the idea of a trajectory as the path of an atom or a fluid element containing an ensemble of atoms is limited in hydrodynamics, and in particular, in the dynamics of a rarefied plasma. Nevertheless, the trajectory of a volume element following (1.1) and (1.2), complemented by an equation of state for $\ddot{\pi}$ and an energy balance equation for T is mathematically well defined as the solution of

$$\frac{\mathrm{d}\boldsymbol{v}}{\mathrm{d}t} = \boldsymbol{F}(\boldsymbol{x}, \boldsymbol{v}, \nabla\ddot{\pi}, t)\,, \quad \frac{\mathrm{d}\boldsymbol{x}}{\mathrm{d}t} = \boldsymbol{v}(\boldsymbol{x}, t)\,. \tag{2.1}$$

Let us assume that on the compact domain D $\boldsymbol{F}$ is continuous for a given time interval and that the system (2.1) obeys a Lipschitz condition. Then a unique solution of (2.1),

$$\boldsymbol{x} = \boldsymbol{x}(\boldsymbol{a}, t)\,, \quad \boldsymbol{x}(\boldsymbol{a}, t_0) = \boldsymbol{a}\,, \tag{2.2}$$

exists. If, in addition, the partial derivatives $\partial v_i/\partial x_j$ are continuous on D it follows that $\boldsymbol{x}$ is continuously differentiable with respect to the initial position $\boldsymbol{a}$ and the inverse mapping also exists. Hence, $\boldsymbol{x}(\boldsymbol{a}, t)$ is a diffeomorphism on the manifold of initial positions $D_0 = \{\boldsymbol{a}\}$. Locally the existence of the inverse of the mapping (2.2) is assured if the density ratio $\varrho(\boldsymbol{a}, t)/\varrho(\boldsymbol{a}, t_0)$ remains finite in D_0 since then from (1.3) $J \neq 0$ follows. On the other hand nothing can be concluded from $J(\boldsymbol{x}, t) = 0$ with $\boldsymbol{x}$ belonging to a subset in D_0 of zero Lebesque measure: the mapping may or may not have an inverse (the two mappings $u = x$, $v = y$, $w = z^3$ and $u = x$, $v = y$, $w = z^2$ both have $J(x, y, 0) = 0$, but of the first the inverse exists, whereas for the second does not).

A more complex question is that of global existence of the inverse mapping. It is not sufficient that on a compact domain $J \neq 0$ everywhere. An example illustrating this is the following: $u = xy$, $v = (x^2 + y^2)/2$ in the domain $\varepsilon \leqq x^2 + y^2 \leqq 1$, $\varepsilon > 0$. The Jacobian is $J = x^2 + y^2 > 0$, but the two points (x, y), $(-x, -y)$ have the same image (u, v). In particular, each point (u_0, v_0) on the boundary is the image of two boundary points $(\pm x_0, \pm y_0)$. However, if there is one boundary point (u_0, v_0) of D which is the image of exactly one boundary point (x_0, y_0) the existence of a global inverse mapping is guaranteed. More precisely the following theorem holds:

If $\boldsymbol{x}(\boldsymbol{a}, t)$ is a continuously differentiable mapping on the compact domain D_0 (I) which maps the interior of D_0 onto the interior of the image of D_0 (II); if there exists one boundary point $\boldsymbol{x}_0$ which is the only image of $\boldsymbol{a}_0$ with $J(\boldsymbol{a}_0, t) \neq 0$ (III), and if $J \neq$ holds everywhere in the interior of D_0 (IV), then $\boldsymbol{x}(\boldsymbol{a}, t)$ is a diffeomorphism in the interior of D_0.

The theorem gives a sufficient condition for the existence of $\boldsymbol{x}^{-1}$. Its proof is nearly evident. The existence of the inverse in a sufficiently small neighbourhood of each point $\boldsymbol{x}$ is assured by $J(\boldsymbol{a}, t) \neq 0$ since the inverse is obtained by solving a linear system of equations having determinant J taken in an appropriate point $\boldsymbol{a}'$. Furthermore, uniqueness follows from continuity and Heine-Borel's theorem.

A topological mapping and a diffeomorphism in particular have some interesting consequences for an arbitrary fluid volume $V_0 \subset D_0$, namely:

α) A trajectory starting from the interior of V_0 ends in an interior point of V_t, and a boundary point of V_0 remains a boundary point of V_t.

β) The degree of connection of V_t is an invariant of fluid motion.

In fact, properties α and β are easily shown to be consequences of the continuity of mapping $\boldsymbol{x}(\boldsymbol{a}, t)$, i.e. that open neighbourhoods are mapped onto open neighbourhoods and closed ones onto closed ones, and the existence of $\boldsymbol{x}^{-1}$. The situation of a few cases is illustrated by Figure 1. They have some surprising implications for applied fluid dynamics.

3. Applications

As a first case illustrating properties α and β we consider the implosion of a hollow pellet of DT by a laser or a heavy ion beam [7, 8]. In this case the implosion dynamics is well described by ideal hydrodynamics. As a consequence, eventual shocks

converging to the pellet center or originating from there after the collapse degenerate to discontinuity interfaces moving through the fluid (see Figure 2). At the instant of shock reflection or when the shock is generated at the center due to stagnation of the rarefaction wave the density and flow velocity are continuous in a whole region including the center because the density jump from ϱ_0 to ϱ_1 in a shock is bounded by the relation

$$\varrho_1(x,t) = \varkappa \varrho_0(x,t)\,, \quad \varkappa < \infty\,; \quad \varkappa = \frac{(\gamma+1)M^2}{(\gamma-1)M^2+2}\,. \tag{3.1}$$

Here $\varkappa$ indicates the compression ratio of the shock in an ideal gas as a function of the Mach number M and the adiabatic exponent γ.

Now, consider an arbitrary volume V_0 lying inside the DT pellet and enclosing the void, i.e. the region H of density $\varrho = 0$. In order to make the density distribution unique in V_0 to the eventual discontinuity positions the lower value of ϱ is assigned. It is easily seen that the Lagrange mapping $x(a,t)$ on V_0 is topological, i.e. continuous and biunique, as long as ϱ is bounded regardless of whether there are discontinuities present in ϱ or not. As a consequence, property β applies: The hole H may degenerate to a point of density $\varrho = 0$; however, it persists for all times.

It has to be mentioned that numerical calculations which reproduce this singularity to a sufficient precision are extremely time consuming. Fortunately, there is a model of homogeneous pellet compression which is relevant in cosmology as well as in inertial confinement fusion [9] and is accessible to an analytical treatment. The basis of the model consists in the assumptions of one-dimensional geometry (plane, cylindrical, spherical) and that in the process of compression or expansion each fluid element is compressed or rarefied by the same fraction $f(t)$,

$$\varrho(a,t) = \varrho_0(a) \cdot f(t)\,, \tag{3.2}$$

with a the Lagrangian coordinate. From this relation in spherical geometry one deduces immediately

$$\begin{aligned} r &= a h(t)\,, \quad \varrho(a,t) = \varrho_0(a)\, h^{-3}\,, \\ T(a,t) &= T_0(a)\, h^{-2}\,, \\ p(a,t) &= p_0(a)\, h^{-5}\,, \quad f = h^{-3}\,. \end{aligned} \tag{3.3}$$

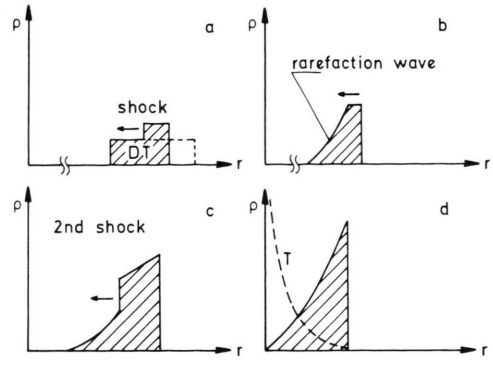

Fig. 2. Implosion scenario in inertial confinement fusion: (a) first shock, (b) acceleration phase, (c) second, spark forming shock, (d) central spark formation.

For a spherical shell of outer and inner initial radii of a_2 and a_1 and isentropic flow with $\gamma = 5/3$, $p_0 \varrho_0^{-\gamma} = p_0(a_2)\, \varrho_0^{-\gamma}(a_2)$ is explicitely calculable:

$$\begin{aligned} h(t) &= \left(1 - \frac{t^2}{t_c^2}\right)^{1/2}\,, \quad t_c^2 = \frac{1}{3 s_2^2}(a_2^2 - a_1^2)\,, \\ s_2^2 &= \gamma \frac{p_0(a_2)}{\varrho_0(a_2)}\,. \end{aligned} \tag{3.4}$$

If the shell is initially at rest ($v(t=0) = 0$) the dynamic quantities are easily deduced to be distributed in space as follows,

$$\begin{aligned} \varrho_0(a) &= \varrho_2 \left(\frac{a^2 - a_1^2}{a_2^2 - a_1^2}\right)^{3/2}\,, \quad T_0(a) = T_2 \frac{a^2 - a_1^2}{a_2^2 - a_1^2}\,, \\ p_0(a) &= p_2 \left(\frac{a^2 - a_1^2}{a_2^2 - a_1^2}\right)^{5/2}\,. \end{aligned} \tag{3.5}$$

Prior to the instant of collapse $t = t_c$ the hole inside the pellet does not close no matter how small the outer radius $r_2 = a_2 h(t)$ of the shell has become. Only when r_2 has reduced to zero at $t = t_c$ pellet and void degenerate to a singularity in accordance with the assertions in Section 2.

As a second example we consider the problem of foil acceleration and impact onto a solid wall [10]. A mathematically precisely equivalent problem is the following version of the historical Gay-Lussac experiment: A box is subdivided into two chambers one of which is filled with a compressible fluid and the other one is empty [11]. When the gas is released by instantaneously removing the separating wall a rarefaction wave develops, and matter is

accelerated into vacuum. When the gas arrives at the opposite wall it is stopped; a strong shock then originates from the wall and propagates backward into the counterstreaming fluid. Again a singular point exists, this time being located at the solid wall. If the rarefaction wave is such that at its front both the density and the sound speed drop to zero, ϱ will remain zero for all times at the wall, the reason being exactly the same as in the former case of pellet compression. To recognize this it is sufficient to mirror the Gay-Lussac (or the foil impact) experiment in the plane of the solid wall. Then a hole of the shape of an infinite slit results which is topologically equivalent to the spherical case. If the fluid follows the ideal gas law the front of the fluid before the impact moves at the constant velocity of $v_{\max}$,

$$v_{\max} = \frac{2}{\gamma - 1} s_0 , \quad s_0^2 = \gamma \frac{p_0}{\varrho_0} . \tag{3.6}$$

At the instant of impact a finite pressure builds up at zero density which means that the temperature jumps from zero to infinity. The history of density evolution is presented in Figure 3. After a while the returning shock is reflected at the left wall of the box. By bouncing forth and back in the box it attenuates due to reflection and finally decays.

It is interesting to look at the consequences of the singular point at the second wall for thermalization of the gas. A comparison of the dynamics in the ideal case with that of viscosity and heat conduction included shows [11] that more than 95% of the final entropy increase ΔS,

$$\Delta S = N k \ln (1 + V_2/V_1) \tag{3.7}$$

originates from the shock wave and that the short time behaviour (i.e. the first few shock reflections) is perfectly described by the ideal gas dynamics. It is only for final thermalization and the long time behaviour that heat conduction plays a role; without the latter no final equalization of temperature would be achieved. Dissipation due to viscosity in the ideal gas plays only a minor role. In ideal hydrodynamics the main dissipation or entropy production is produced by the shock discontinuity [11].

The final case we study here is that of an infinite ideal gas at rest of constant density and temperature in which a spherical shock is converging from infinity [12]. Regardless of how weak such a shock initially was it develops into a strong one as it approaches its geometrical center. As a consequence, it becomes asymptotically self-similar. This property is a consequence of the absence of any relevant length scale in contrast to the pellet implosion given by (3.2)–(3.5), in which all quantities depend on r (or a) and t separately. At the center the density behaves in the following way:

$$\begin{aligned} &\varrho(t) = \varrho_0 \quad \text{for} \quad t < t_c , \quad \varrho(t_c) = \alpha > \varrho_0 , \\ &\varrho(t) = 0 \quad \text{for} \quad t > t_c . \end{aligned} \tag{3.8}$$

For $\gamma = 5/3$ $\alpha = 32.0\,\varrho_0$ is obtained [13]. Here we have one of the rare cases in physics in which a function assumes a discontinuous value at one instant $t = t_c$ only. The mapping $\boldsymbol{x}(\boldsymbol{a}, t)$ is again topological; however, nothing can be concluded about the existence or nonexistence of a singularity. In fact, in contrast to the former case of foil impact in the present example the behaviour at the point of shock reflection depends on geometry. When the same shock is launched in plane geometry in a gas of constant density, after reflection from a solid wall, the gas density including the points at the wall is uniform everywhere.

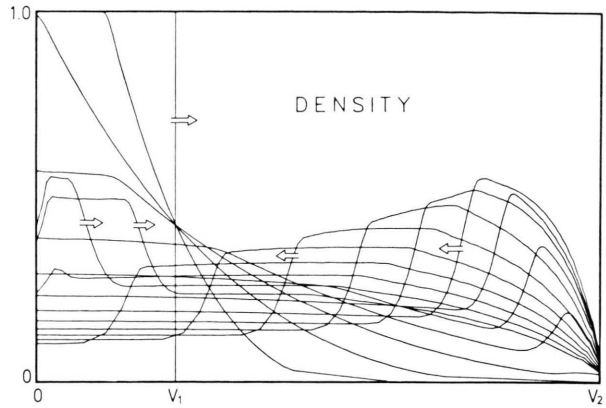

Fig. 3. Foil impact or Gay-Lussac experiment. An ideal gas initially fills volume V_1. After the gas expands through volume V_2 and reaches the solid wall, a strong backrunning shock forms. The density remains zero for all times, and the temperature diverges, just at the wall.

4. Discussion and Conclusion

We have seen through the concept of trajectories that in ordinary fluid dynamics fluid elements are

mapped onto fluid elements as a function of time. In this way a diffeomorphism is induced by the flow. Physically the existence of trajectories is limited by particle diffusion which leads to a finite distinguishibility lifetime of fluid elements. In a fluid composed of neutral particles the mutual forces are of short range type. Collective behaviour therefore takes place on a space scale larger than the mean free path λ. Below this value no structure exists at finite temperature and a fluid description with the help of conservation equations of type (1.1) is no longer useful. On the other hand, the situation is different when the fluid is composed of charged particles as is the case for a plasma. Here the minimum extension of collective behaviour is given by the Debye length λ_D which may be smaller than λ by orders of magnitude (e.g. in a collisionless plasma). From kinetic equations, moment equations are derived which often assume exactly the same structure as the corresponding hydrodynamic balance equations for momentum and energy. This is not so by chance. In a fluid of short range forces for example a pressure difference can manifest itself only by collisions. However, when the particles exhibit long range interactions a pressure gradient can transmit momentum by interacting with the collective fields. However there is a difference relative to standard fluid dynamics when $\lambda_D \ll \lambda$ holds in so far as a Lagrangian description exists only mathematically owing to the short lifetime of a material point and the concept of a trajectory becomes fictitious from the physical point of view. Nevertheless, all topological aspects apply equally well since these are based on mathematical structures only, and mathematically trajectories are well defined even in such cases.

It has been shown and illustrated by examples that in the case fluid flow represents a homeomorphism some very general topological properties can be deduced which, as in the case of hypervelocity foil impact or of the Gay-Lussac experiment lead to surprising results, for instance on the absence of thermalization in a finite time. In this context it has further become evident that mathematical discontinuities, so called weak solutions, may exhibit a strongly dissipative character.

In connection with the investigation of trajectories the phenomenon of bifurcation or breaking has to be mentioned: a single fluid element splits into two separate elements which follow then two different trajectories. In laser plasma interaction wave breaking occurs in resonantly excited nonlinear electron plasma waves [14]. When a Langmuir wave grows higher and higher in amplitude the concomitant compression enthalpy may increase to such a level that part of a fluid element when moving through its own electrostatic potential is reflected. This mechanism is very effective in destroying fluid trajectories. It was further recognized that the knowledge of the physical trajectories very much depends on the lifetime τ_1 of the single fluid element. The formulae given for τ_1 apply to regular flow. In the case of strong turbulence it is well known that after some time a regular volume element may assume a fractal structure. In fact by measuring the ratio perimeter P versus square root of the area A of a large number of clouds the relation

$$P \sim \sqrt{A^{1.35}}$$

was found [15]. Especially this phenomenon is perhaps best suited to underline the discrepancy between the mathematical trajectories of fluid elements and the real particle orbits when τ_1 becomes small.

[1] A. J. Corin and J. E. Marsden, A mathematical introduction to fluid mechanics, Springer-Verlag, Berlin 1979. J. Wick, Math. Methods Appl. Sci. **1**, 383 (1979).
[2] Yung-Chen Lu, Singularity theory, catastrophe theory, Springer-Verlag, New York 1980.
[3] L. Lichtenstein, Grundlagen der Hydromechanik (Principles of Hydromechanics), Springer-Verlag, Berlin 1929, reprint 1968. Anatole Beck, Continuous Flows in the Plane, Springer-Verlag, Berlin 1974. – F. Matyas, Die Darstellung physikalischer Strömungen als topologische Abbildung bewegter mathematischer Kontinua (representation of physical flows in terms of the topological mapping of moving continuous domains) in „Festschrift zum 60. Geburtstag von Prof. Dr.-Ing. Erich Truckenbrodt", Munich 1977.
[4] R. Balescu, Equilibrium and nonequilibrium statistical mechanics, John Wiley, New York 1975.
[5] R. G. Evans, Plasma simulation using fluid and particle models, in laser-plasma interactions 3, Proc. 29th SUSSP, 1985, p. 247–278, and refs. therein.
[6] D. A. Tidman and N. A. Krall, Shock Waves in Collisionless Plasmas, Wiley-Interscience, New York 1971. G. Härendel, G. Paschmann, Interaction of the Solar Wind with the Dayside Magnetosphere, in

Magnetospheric Plasma Physics, A. Nishida ed., Reidel, Dordrecht 1982, p. 68–81.
[7] P. Mulser, Plasma Phys. and Controlled Fusion **28,** 203 (1986).
[8] R. Arnold and J. Meyer-ter-Vehn, Rep. Prog. Phys. **50,** 559 (1987) and Max-Planck-Institut für Quantenoptik report MPQ-113 (1986).
[9] R. E. Kidder, Nucl. Fusion **16,** 405 (1976).
[10] A. E. M. Maaswinkel, K. Eidmann, R. Sigel, and S. Witkowski, Optics Comm. **51,** 255 (1984); see also [9] therein.
[11] P. Mulser and B. Kärcher, to be published.
[12] G. Guderley, Luftfahrtforschung **19,** 302 (1942).
[13] J. Meyer-ter-Vehn and C. Schalk, Z. Naturforsch. **37 a,** 955 (1982).
[14] P. Mulser, K. Takabe, and K. Mima, Z. Naturforsch. **37 a,** 208 (1982); P. Mulser and H. Schnabl, Laser and Particle Beams **1,** 379 (1983); A. Bergmann and H. Schnabl, to be published.
[15] S. Lovejoy, Science **216,** 185 (1982).